JACS
JOURNAL OF THE AMERICAN CHEMICAL SOCIETY

Article

pubs.acs.org/JACS

Mechanism of the Palladium-Catalyzed Arene C−H Acetoxylation: A Comparison of Catalysts and Ligand Effects

Amanda K. Cook and Melanie S. Sanford*

Department of Chemistry, University of Michigan, 930 North University Avenue, Ann Arbor, Michigan 48109, United States

Supporting Information

ABSTRACT: This article describes detailed mechanistic studies focused on elucidating the impact of pyridine ligands on the Pd-catalyzed C−H acetoxylation of benzene. Three different catalysts, $Pd(OAc)_2$, $Pd(OAc)_2$/pyridine (1:1), and $Pd(OAc)_2$/pyridine (1:2), are compared using a combination of mechanistic tools, including rate and order studies, Hammett analysis, detailed characterization of catalyst resting states, and isotope effects. The data from these experiments implicate C−H activation as the rate-limiting step in all cases. The major difference between the three catalysts is proposed to be the resting state of Pd. Under the reaction conditions, $Pd(OAc)_2$ rests as an acetate bridged dimer, while the $Pd(OAc)_2$/pyridine (1:2) catalyst rests as the monomer $(pyridine)_2Pd(OAc)_2$. In contrast, a variety of experiments suggest that the highly active catalyst generated from the 1:1 combination of $Pd(OAc)_2$ and pyridine rests as the dimeric structure $[(pyridine)Pd(OAc)_2]_2$.

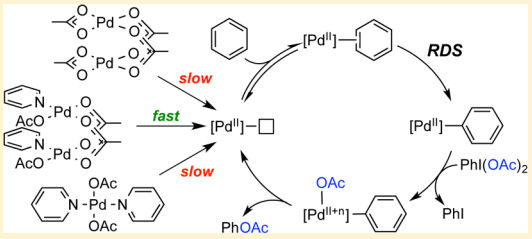

INTRODUCTION

Over the past 15 years, there have been major advances in the field of Pd-catalyzed C−H functionalization.[1] Palladium catalysis enables the introduction of a diverse array of functional groups, often in the context of complex organic molecules.[2] However, the vast majority of synthetic[1,2] and mechanistic[3] efforts in this area have focused on substrates bearing directing groups (DG). These directing groups render the reactions kinetically fast as well as highly site-selective for C−H functionalization proximal to the directing groups (Scheme 1a).[3p,4] In contrast, analogous non-directed Pd-catalyzed C−H functionalization processes have been much less developed in terms of both synthetic applications[5] and mechanistic analysis[3f,6] (Scheme 1b). The identification of efficient and selective catalysts for non-directed C−H functionalization is of particular importance,[7] because many synthetic targets do not contain directing groups.

Scheme 1. Comparison of Directed and Non-Directed C−H Functionalization

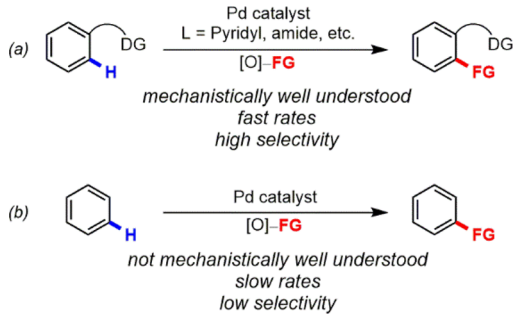

Over the past several years, our group has focused on developing Pd catalysts for the non-directed C−H acetoxylation of arenes.[8] The Pd-catalyzed C−H acetoxylation of benzene was originally reported in the 1970s using simple Pd salts and oxidants such as $K_2Cr_2O_7$ and $K_2S_2O_8$.[9−11] While these early studies provided proof-of-principle for the feasibility of this transformation, the catalyst turnover numbers (TON) were too low for practical utility (typically ranging between <1 and 7). In 1996, Crabtree reported that the combination of $Pd(OAc)_2$ as catalyst and $PhI(OAc)_2$ as oxidant afforded dramatically improved results, with up to 127 turnovers in the C−H acetoxylation of naphthalene.[12] More recently, our group has demonstrated that the rate and TON of Crabtree's reaction can be increased dramatically through the use of pyridine (pyr) as a supporting ligand.[8c] The ratio of $Pd(OAc)_2$ to pyridine was critical in this system, with a 1:1 ratio proving optimal. This second-generation catalyst system provided an approximately 10-fold increase in reaction rate versus $Pd(OAc)_2$, and TONs of >4500 were achieved (Scheme 2). In addition, the site

Scheme 2. Pyridine Ligand Effects in the Pd-Catalyzed C−H Acetoxylation of Benzene

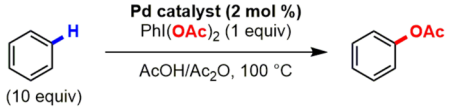

catalyst:	$Pd(OAc)_2$	$Pd(OAc)_2$ + Pyr (1:1)	$Pd(OAc)_2$ + Pyr (1:2)
yield after 4 h:	12%	68%	7%

Received: January 8, 2015
Published: February 23, 2015

DOI: 10.1021/jacs.5b00238
J. Am. Chem. Soc. 2015, 137, 3109−3118

selectivity of this transformation could be tuned through modification of the pyridine ligand.[8a] Despite these advances, the mechanistic role of the pyridine ligand remains poorly understood. Notably, similar pyridine effects have been observed in related Pd-catalyzed C−H functionalization[13] and oxidation reactions,[14] underscoring the significance of mechanistic understanding of ligand effects in these transformations.

This report describes a detailed mechanistic investigation focused on elucidating the impact of pyridine ligands on Pd-catalyzed benzene C−H acetoxylation. We compare three catalyst systems, $Pd(OAc)_2$, $Pd(OAc)_2$/pyridine (1:1), and $Pd(OAc)_2$/ pyridine (1:2), using a combination of mechanistic tools, including rate and order studies, Hammett analysis, detailed characterization of catalyst resting states, and isotope effects. These investigations provide insights into the similarities and differences between the three catalyst systems that explain their dramatically different reactivities.

RESULTS AND DISCUSSION

Mechanistic Investigation of the $Pd(OAc)_2$-Catalyzed C−H Acetoxylation of Benzene. We first assessed the order in Pd for the $Pd(OAc)_2$ catalyst system. In Crabtree's original study, a half-order kinetic dependence on Pd was observed.[12a] This result was rationalized based on a resting state dimer, $[Pd(OAc)_2]_2$, that breaks up into monomeric $Pd(OAc)_2$ to effect catalysis. However, the conditions developed in our lab are somewhat different than those reported by Crabtree (e.g., different concentration of benzene, different solvent system). Thus, we needed to establish whether the same kinetic dependence on Pd is observed in our system.

The method of initial rates was used to determine the rate of product formation as a function of Pd concentration over a concentration range of 0.28−56 mM. The reactions were monitored using GC-FID and were run to approximately 10% conversion. Hexafluorobenzene was employed as a co-solvent in order to mitigate changes in the polarity of the reaction medium upon varying the concentration of benzene (during benzene order studies, *vide infra*). Under our reaction conditions, the $Pd(OAc)_2$-catalyzed C−H acetoxylation of benzene showed a half-order dependence on Pd (0.49 ± 0.06), analogous to that observed by Crabtree (see Figure S23 in the Supporting Information). This is consistent with the Pd resting as a dimer in our system.

To further probe the impact of Pd aggregation state, we examined the kinetic order in Pd using $Pd(OTFA)_2$ (OTFA = trifluoroacetate) as the catalyst. In contrast to $Pd(OAc)_2$, $Pd(OTFA)_2$ is known to exist as a monomer in organic solvents.[15] Thus, we predicted that a first-order dependence on [Pd] should be observed with this catalyst. Indeed, under otherwise analogous conditions, the $Pd(OTFA)_2$-catalyzed C−H acetoxylation of benzene was first order in [Pd] (1.0 ± 0.1; see Figure S25). Notably, at 5.6 mM [Pd], the rate of C−H acetoxylation using $Pd(OTFA)_2$ is almost 4-times faster than with $Pd(OAc)_2$ (Δ[PhOAc]/Δt = 6.5 mM/h for $Pd(OTFA)_2$ and Δ[PhOAc]/Δt = 1.7 mM/h for $Pd(OAc)_2$).

We next assessed the kinetic order of the $Pd(OAc)_2$-catalyzed reaction in benzene and $PhI(OAc)_2$. The order in benzene was determined by varying the concentration of benzene from 0.56 to 2.8 M. Hexafluorobenzene was used as a co-solvent, and the sum of the volumes of C_6H_6 and C_6F_6 was held constant during these experiments in order to minimize solvent effects on the observed rates. The order in $PhI(OAc)_2$ was determined by varying the concentration of $PhI(OAc)_2$ from 140 to 840 mM. Under these conditions, the reaction is approximately first order in benzene (1.5 ± 0.3) and zero order (0.1 ± 0.1) in $PhI(OAc)_2$ (Figures S18 and S21).

Finally, the kinetic isotope effect (KIE) was determined by comparing the initial reaction rate with C_6H_6 to that with C_6D_6. A KIE (k_H/k_D) of 4.5 ± 0.4 was obtained from these experiments (Figure S19). This value is similar to that observed under Crabtree's conditions (k_H/k_D = 4.1)[12a] and is consistent with a 1° isotope effect.[16]

On the basis of all of the data presented above, we propose the catalytic cycle in Scheme 3 for the $Pd(OAc)_2$-catalyzed C−H acetoxylation of benzene. The mechanism begins with a dimeric Pd^{II} precatalyst, $[Pd(OAc)_2]_2$ (**1a**), as the resting state. Complex **1a** undergoes reversible dissociation into the monomer **1b**, which lies on the catalytic cycle. C−H activation of benzene at **1b** is the rate-determining step (RDS) and forms the Pd^{II}-aryl intermediate **2**. This complex is then oxidized by $PhI(OAc)_2$ to form a high-valent Pd intermediate **3**, which undergoes reductive elimination to release PhOAc[17] and regenerate **1b**.

Scheme 3. Proposed Mechanism of the $Pd(OAc)_2$-Catalyzed C−H Acetoxylation of Benzene

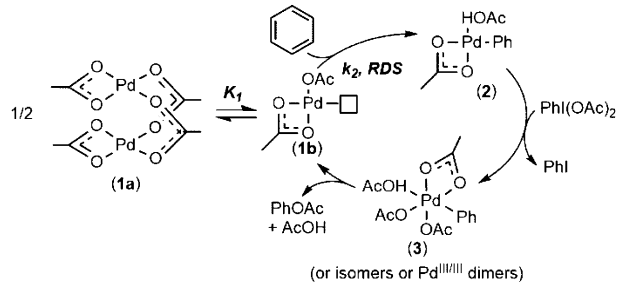

The rate expression for this mechanism can be derived as shown below in eqs 1−3. This rate expression is fully consistent with the experimental data, as it predicts a half-order dependence on Pd, a first-order dependence on benzene, and a zero-order dependence on $PhI(OAc)_2$. Additionally, since C−H activation is the RDS, a 1° KIE is expected.

$$\text{rate} = \frac{\mathrm{d}(\text{PhOAc})}{\mathrm{d}t} = k_2[\mathbf{1b}][\text{benzene}] \quad (1)$$

$$K_1 = \frac{[\mathbf{1b}]}{[\mathbf{1a}]^{1/2}} \quad (2)$$

$$\text{rate} = K_1 k_2 [\mathbf{1a}]^{1/2}[\text{benzene}] \quad (3)$$

Mechanistic Investigation of the $Pd(OAc)_2$/Pyr (1:2)-Catalyzed C−H Acetoxylation of Benzene. We next studied the catalyst generated upon combining a 1:2 ratio of $Pd(OAc)_2$ to pyridine (pyr). To assess the resting state of Pd during catalysis, the reaction was monitored by ^{1}H NMR spectroscopy.[18] The only Pd species observed at the beginning (Figure 1a), middle (Figure 1b), and end (Figure 1c) of the C−H acetoxylation reaction is $(pyr)_2Pd(OAc)_2$ (**4**).[19] The identity of **4** was verified via independent synthesis of this complex (Figure 1d).[20] These data implicate **4** as the catalyst resting state in this system.

The lability of the pyridine ligands in complex **4** was assessed using rotating frame nuclear Overhauser effect NMR spectroscopy (ROESY). As shown in Figure 2, exchange between free

DOI: 10.1021/jacs.5b00238
J. Am. Chem. Soc. 2015, 137, 3109−3118

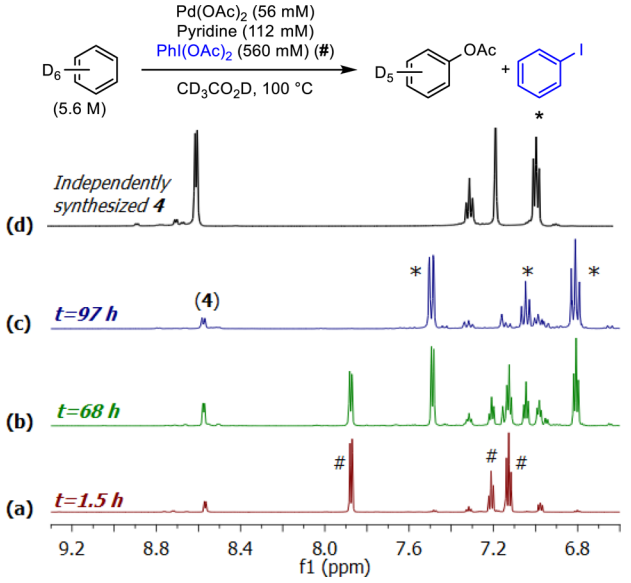

Figure 1. C−H acetoxylation of benzene monitored by ^{1}H NMR spectroscopy (aromatic region shown) using $Pd(OAc)_2$/pyr (1:2) as catalyst. The red spectrum (a) was acquired after heating for 1.5 h, the green spectrum (b) after heating for 68 h, and the blue spectrum (c) after heating for 97 h. *PhI (consumed oxidant) peaks. #$PhI(OAc)_2$ peaks.

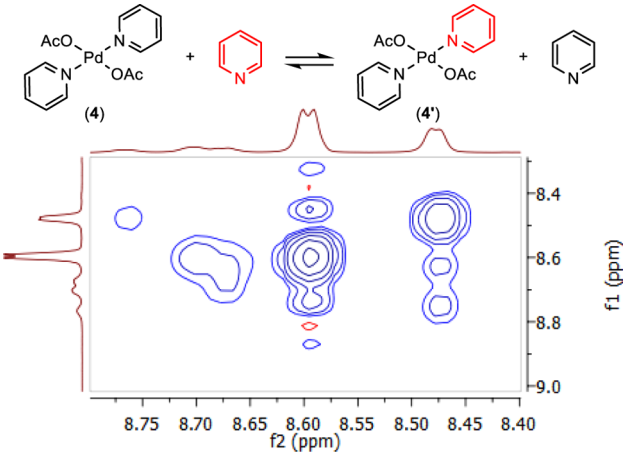

Figure 2. ROESY NMR experiment showing exchange between free (8.48 ppm) and bound (8.59 ppm) pyridine. Spectrum acquired in C_6D_6/CD_3CO_2D (1:1) at 80 °C.

and bound pyridine is observed at 80 °C (20 °C below the temperature used for catalytic C−H acetoxylation). This demonstrates the feasibility of pyridine ligand dissociation/exchange during catalysis.

Using the method of initial rates, we next determined the order of the reaction in each reagent. Importantly, all of these experiments were conducted with a Pd:pyr ratio of 1:2 (i.e., no extra pyidine was added to the reactions). Interestingly, this reaction showed a half-order dependence on [Pd] (0.53 ± 0.07; Figure 3),[21] despite the fact that the catalyst resting state appears to be a monomer.[22] In addition, a first-order dependence on [benzene] (1.01 ± 0.07; Figure 4) and a zero-order dependence on [$PhI(OAc)_2$] (−0.08 ± 0.04; Figure 5) were observed. The value of k_H/k_D for C_6H_6/C_6D_6 was 3.6 ± 0.3 with this catalyst system (Figure S37). Finally, a Hammett plot was constructed by examining the initial reaction

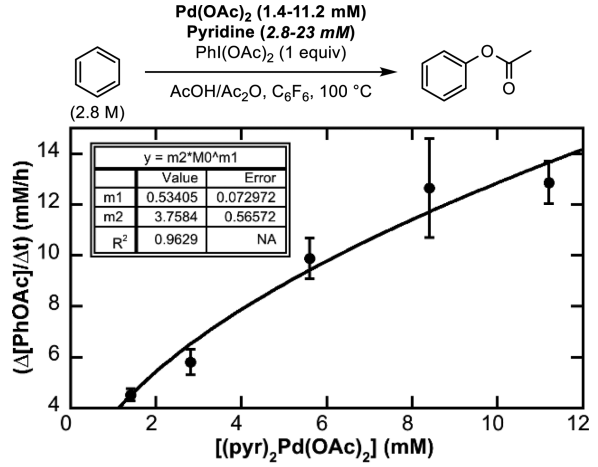

Figure 3. Plot of initial rate versus [Pd] with the $(pyr)_2Pd(OAc)_2$ catalyst in **Regime 1**.

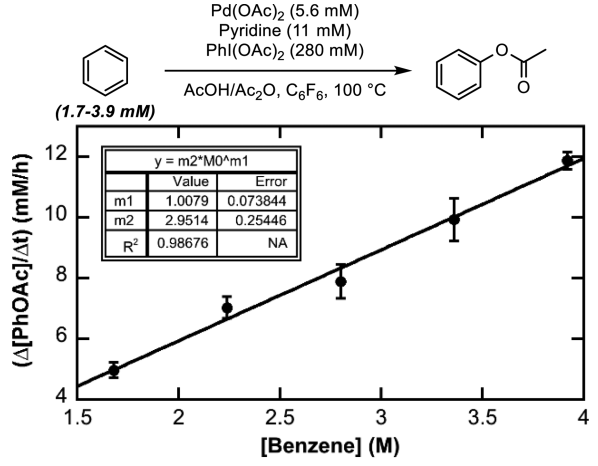

Figure 4. Plot of initial rate versus [benzene] with the $(pyr)_2Pd(OAc)_2$ catalyst in **Regime 1**.

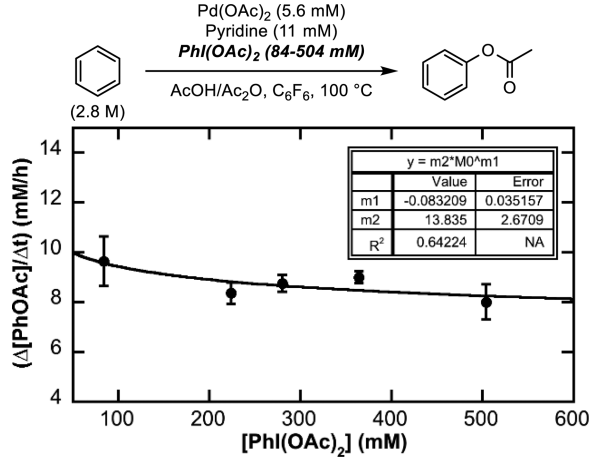

Figure 5. Plot of initial rate versus [$PhI(OAc)_2$] with the $(pyr)_2Pd(OAc)_2$ catalyst in **Regime 1**.

rate with a series of 3- and 4-substituted pyridine derivatives. As shown in Figure 6, a Hammett ρ value of +0.64 was obtained, indicative of increasing reaction rate with more electron-deficient pyridine ligands.

DOI: 10.1021/jacs.5b00238
J. Am. Chem. Soc. 2015, 137, 3109−3118

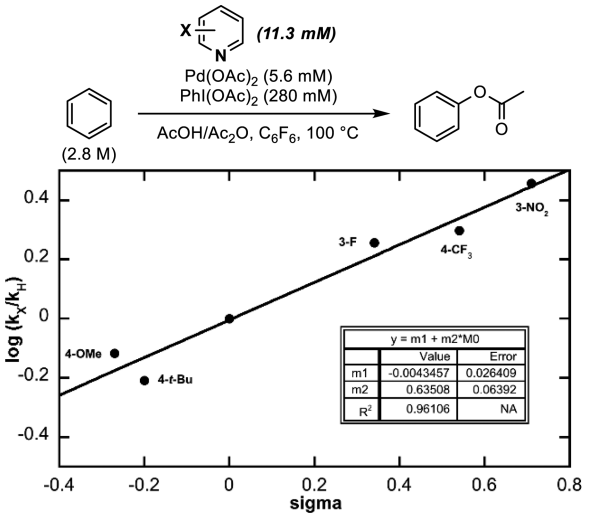

Figure 6. Hammett plot showing the effect of pyridine electronics for the $(pyr)_2Pd(OAc)_2$ catalyst in **Regime 1**.

Scheme 4. Proposed Mechanism for the $(pyr)_2Pd(OAc)_2$-Catalyzed C−H Acetoxylation of Benzene

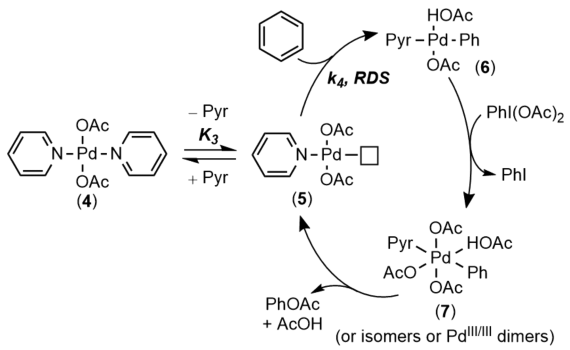

Based on the data discussed above, we propose the mechanism outlined in Scheme 4 for the $Pd(OAc)_2$/pyr (1:2) catalyst system. The NMR data in Figure 1 implicate monomeric complex **4** as the catalyst resting state. This complex then undergoes reversible pyridine dissociation to generate monopyridine complex **5**. The ROESY experiment in Figure 2 supports the feasibility of this step. The positive Hammett ρ value is also consistent, as more electron-deficient pyridine ligands should provide a more favorable equilibrium toward the on-cycle intermediate **5**. C−H activation at **5** to generate **6** is then the RDS. The observation of a first-order dependence on benzene and a 1° KIE is further consistent with this proposal. Finally, $2e^-$ oxidation of **6** would form **7** (or an isomer thereof), and C−O bond-forming reductive elimination would release PhOAc and regenerate **5**.

The rate expression for this sequence is shown in eq 4:

$$\text{rate} = \frac{\text{d(PhOAc)}}{\text{d}t} = k_4[\mathbf{5}][\text{benzene}] \tag{4}$$

Using the equilibrium constant for the dissociation of pyridine from **4** provides eq 5, which can be rearranged to eq 6. Subsitution for [**5**] then provides eq 7.

$$K_3 = \frac{[\mathbf{5}][\text{pyr}]}{[\mathbf{4}]} \tag{5}$$

$$[\mathbf{5}] = \frac{K_3[\mathbf{4}]}{[\text{pyr}]} \tag{6}$$

$$\text{rate} = \frac{k_4K_3[\mathbf{4}][\text{benzene}]}{[\text{pyr}]} \tag{7}$$

On the basis of the expression in eq 7, we would initially anticipate a first-order dependence on [Pd]. However, since all of the kinetic orders were determined under conditions where no exogeneous pyridine is added, we can approximate that [pyr] = [**5**] and hence reduce eq 5 to eq 8. This will be referred to as **Regime 1** for the rest of the discusson. Using this approximation, the rate expression reduces to eq 9, which predicts a half-order dependence on [Pd], first-order dependence on benzene, and zero-order dependence on $PhI(OAc)_2$, which are all in line with experimental observations.

$$K_3 = \frac{[\mathbf{5}]^2}{[\mathbf{4}]}; \quad [\mathbf{5}] = K_2^{1/2}[\mathbf{4}]^{1/2} \tag{8}$$

$$\text{rate} = k_4K_3^{1/2}[\mathbf{4}]^{1/2}[\text{benzene}] \tag{9}$$

The approximation that [pyr] = [**5**] (**Regime 1**) will break down under conditions where exogeneous pyridine is added to the catalytic reaction. When [pyr] ≫ [**5**] (referred to as **Regime 2** for the remaining discussion), the rate expression in eq 7 should be in operation. Here, a first-order dependence on [Pd], first-order dependence on benzene, and inverse first-order dependence on pyridine are expected.

We next sought to experimentally determine the kinetic orders in [Pd], benzene, and pyr in the presence of added pyridine (**Regime 2**). However, with catalyst **4**, the addition of pyridine resulted in reaction rates that were too slow to measure accurately and reliably, even at elevated temperatures. To address this issue, we moved to the analogous 3-nitropyridine-containing catalyst **4-NO_2**. In **Regime 1**, this catalyst reacts approximately 3-times faster than its pyr analogue (Figure 6), and we hypothesized that this would translate to enhanced reactivity and more reproducible rates in **Regime 2**.

The **4-NO_2**-catalyzed conversion of benzene to phenyl acetate was first examined under **Regime 1** to compare the catalyst resting state and orders in [Pd], benzene, and $PhI(OAc)_2$ to those obtained with catalyst **4**. As shown in Figure 7, the bis-pyridine complex $(3\text{-}NO_2pyr)_2Pd(OAc)_2$ (**4-NO_2**) was the only Pd-containing species detected during catalysis, consistent with this complex as the catalyst resting state. In the absence of added ligand (**Regime 1**), we observed an approximately half-order dependence on [Pd] (0.67 ± 0.03; Figure 8), approximately first-order dependence on benzene (1.4 ± 0.2), and zero-order dependence on $PhI(OAc)_2$ (−0.06 ± 0.05) (Figures S49 and S51). These results are closely analogous to those obtained with catalyst **4** and thus implicate similar mechanisms for **4** and **4-NO_2** in **Regime 1**.

We next evaluated catalyst **4-NO_2** in the presence of exogeneous 3-nitropyridine (28 mM). These conditions correspond to **Regime 2**; thus the rate expression in eq 7 is expected to be operative. Indeed, an approximately first-order dependence on [Pd] (1.2 ± 0.1; Figure 9), approximately inverse first-order dependence on 3-nitropyridine (−1.4 ± 0.1; Figure 10), first-order dependence on benzene (1.0 ± 0.1; Figure S57), and zero-order dependence on $PhI(OAc)_2$ (0.05 ± 0.08; Figure S59) were observed. These results are consistent

DOI: 10.1021/jacs.5b00238
J. Am. Chem. Soc. 2015, 137, 3109−3118

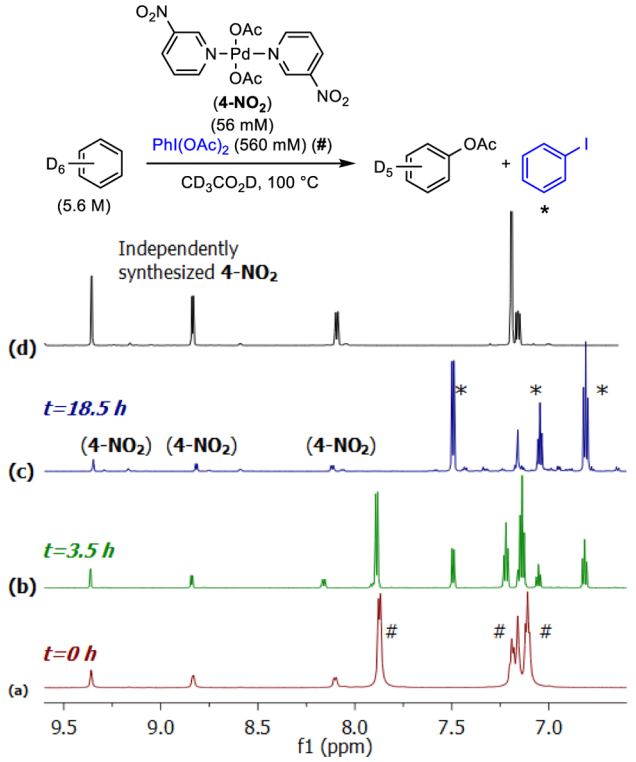

Figure 7. C–H acetoxylation of benzene monitored by ^{1}H NMR spectroscopy (aromatic region shown) using **4-NO$_2$** as catalyst. The red spectrum (a) was acquired prior to heating, the green spectrum (b) after heating for 3.5 h, and the blue spectrum (c) after heating for 18.5 h. *PhI (consumed oxidant) peaks. #PhI(OAc)$_2$ peaks.

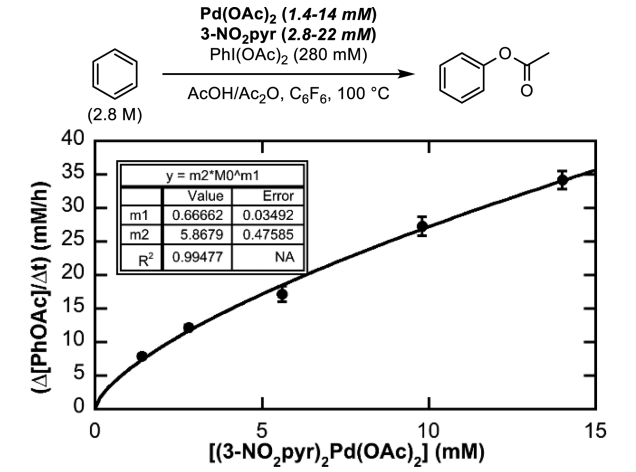

Figure 8. Plot of initial rate versus [Pd] for the (3-NO$_2$pyr)$_2$Pd(OAc)$_2$ catalyst in **Regime 1**.

with the mechanism shown in Scheme 4 as well as the rate expression in eq 7. Notably, these results are analogous to work by Stahl[23] and Hartwig,[24] in which half order in catalyst was obtained in a regime in which ligand dissociation occurs prior to the RDS. In both systems upon addition of exogenous ligand, the catalysts no longer showed half-order dependencies.

Mechanistic Investigation of the Pd(OAc)$_2$/Pyridine (1:1) Catalyst System. Finally, we conducted a detailed investigation of the most active catalyst system, which is generated by combining a 1:1 ratio of Pd(OAc)$_2$ to pyridine. To assess the catalyst resting state under these conditions, we

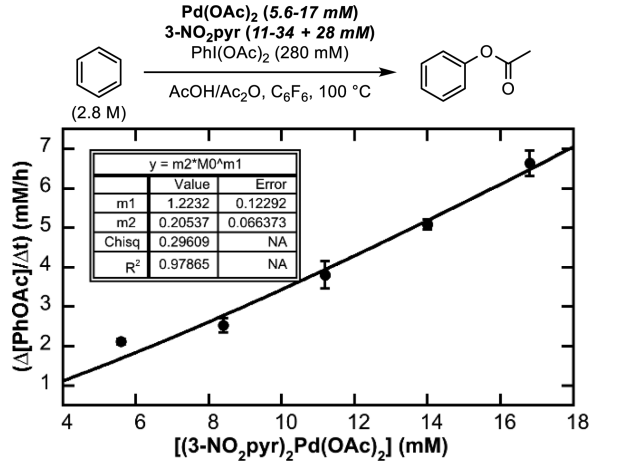

Figure 9. Plot of initial rate versus [Pd] for the (3-NO$_2$pyr)$_2$Pd(OAc)$_2$ catalyst in **Regime 2**.

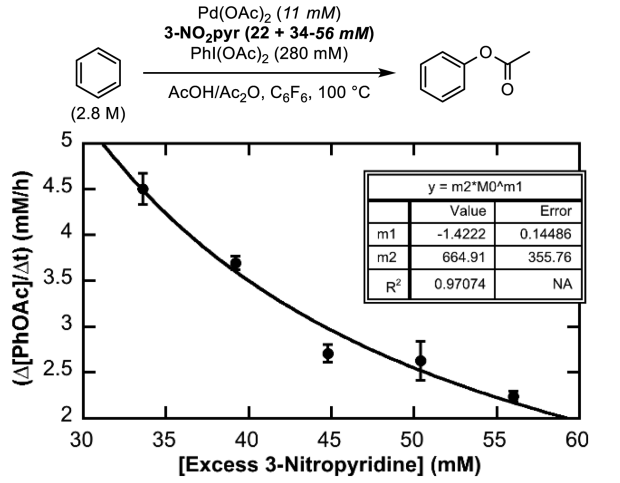

Figure 10. Plot of initial rate versus [excess 3-NO$_2$Pyr] for the (3-NO$_2$pyr)$_2$Pd(OAc)$_2$ catalyst in **Regime 2**.

combined equimolar quantities of pyridine and Pd(OAc)$_2$ in C_6D_6/CD_3CO_2D. ^{1}H NMR spectroscopic analysis at room temperature showed a mixture of two Pd-pyridine adducts: complex **4** [(pyr)$_2$Pd(OAc)$_2$] along with a second species of unknown structure (**8**) (Figure 11). As shown in Figure 12, both complexes **4** and **8** are observed throughout the catalytic reaction. Since the reaction rate under these conditions is significantly higher than that with **4** alone, we propose that **8** is likely the predominant active catalyst (or resting state of the active catalyst) in this system.[25]

As shown in Figure 11, complex **8** could be a monomer (**8a**), dimer (**8b**), trimer (**8c**), or a larger oligomeric structure with a Pd:pyr stoichiometry of 1:1. A diffusion-ordered spectroscopy (DOSY) NMR experiment was performed to obtain the approximate molecular weight of **8** and thus to preliminarily differentiate between these possibilities.[26] This experiment involves generating **8** *in situ* in the presence of a series of different molecules that serve as molecular weight standards. These standards (which include small organic molecules and large Pd complexes) were selected based on three criteria: (i) they represent a wide range of molecular weights (MW), (ii) they are all expected to be unreactive with **8** and with each other, and (iii) they have distinct ^{1}H NMR signals. The DOSY NMR spectrum of this mixture was then obtained at 25 °C in

DOI: 10.1021/jacs.5b00238
J. Am. Chem. Soc. 2015, 137, 3109–3118

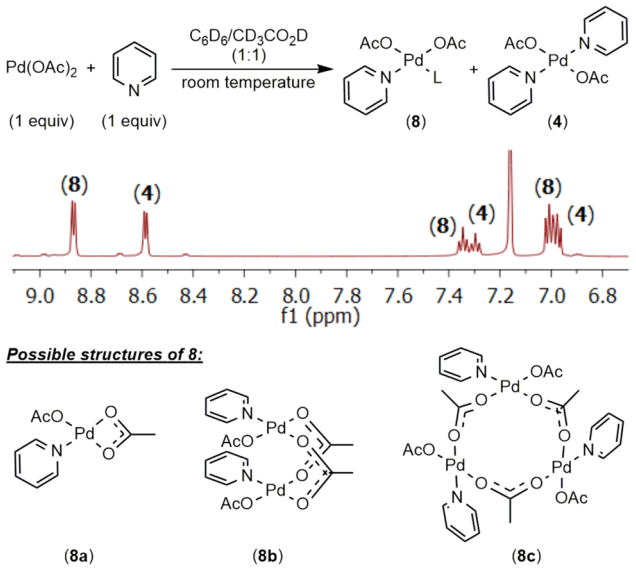

Figure 11. New species (**8**) observed by ^{1}H NMR spectroscopy along with **4** when combining a 1:1 ratio of $Pd(OAc)_2$:pyr.

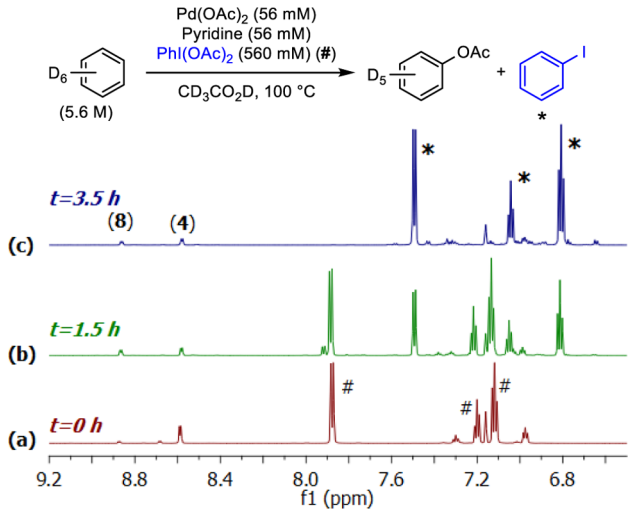

Figure 12. C−H acetoxylation of benzene monitored by ^{1}H NMR spectroscopy (aromatic region shown) using a $Pd(OAc)_2$:pyr ratio of 1:1. The red spectrum (a) was acquired at t = 0, the green spectrum (b) at t = 1.5 h, and the blue (c) at the completion of the reaction (t = 3.5 h). *PhI (consumed oxidant) peaks. #$PhI(OAc)_2$ peaks.

C_6D_6/CD_3CO_2D (1:1). The raw spectrum is provided in Figure S68, and the resulting plot of log(MW) versus log(D) (D = diffusion coefficient) is shown in Figure 13. On the basis of this data, the molecular weight of **8** is calculated to be 755 g/mol (blue data point in Figure 13). This value is in between that of the dimer **8b** (607 g/mol) and the trimer **8c** (911 g/mol). Importantly, the DOSY experiment requires assumptions about the size and shape of the standards compared to **8**; therefore, the calculated MW is only an approximation. Nonetheless, we believe that these data suggest that complex **8** is unlikely to be a monomer (**8a**).

To gain further insights into the structure of **8**, we perfomed an NMR experiment using 1 equiv of $Pd(OAc)_2$ and 0.5 equiv each of two distinct pyridine derivatives (X and Y). If the **8** is a monomer (**8a**), two different complexes should be formed in a 1:1 ratio: $(X)Pd(OAc)_2$ and $(Y)Pd(OAc)_2$. If **8** is a dimer (**8b**),

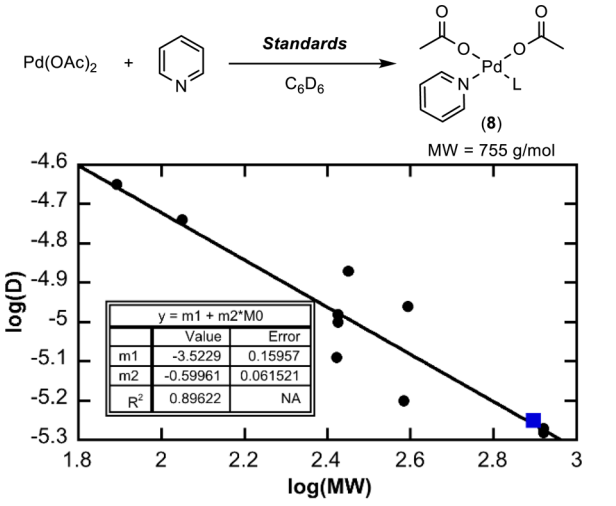

Figure 13. DOSY data used to approximate the molecular weight of $[(pyr)Pd(OAc)_2]_n$ (blue data point) in solution. Standards used are benzene, cyclooctane, 18-crown-6, 4,4′-(t-Bu)$_2$biphenyl, 1,3,5-$(CF_3)_3Ph$, $(pyr)_2Pd(OAc)_2$, $Si(Me)_2(C_6F_5)_2$, and $(IMes)_2Pd(OAc)_2$ (IMes = 1,3-bis(2,4,6-trimethylphenyl)-1,3-dihydro-2*H*-imidazol-2-ylidene).

three compounds are expected in a 1:1:2 ratio: $[(X)Pd(OAc)_2]_2$, $[(Y)Pd(OAc)_2]_2$, and $(X)(Y)Pd_2(OAc)_4$. Finally, if **8** is a trimer (**8c**), four compounds are expected in a 1:1:3:3 ratio: $[(X)Pd(OAc)_2]_3$, $[(Y)Pd(OAc)_2]_3$, $(X)_2(Y)Pd_3(OAc)_6$, and $(X)(Y)_2Pd_3(OAc)_6$ (for a pictorial explanation, see Supporting Information, Section 9).[27] We chose 4-methoxypyridine and 4-*tert*-butylpyridine for X and Y since they are expected to have similar binding affinities to $Pd(OAc)_2$ yet their ^{1}H NMR chemical shifts are well resolved. Upon mixing, the ^{1}H NMR spectrum shown in Figure 14c was obtained (only the signals associated with the 2-position of the pyr derivatives are shown). Both $[(4\text{-OMe-pyr})Pd(OAc)_2]_n$ (see Figure 14a (green) for independently acquired ^{1}H NMR spectrum) and $[(4\text{-}t\text{-Bu-pyr})Pd(OAc)_2]_n$ (see Figure 14b (blue) for independently acquired ^{1}H NMR spectrum) are observed along with signals associated with at least one additional compound. Since >2 distinct species are detected, monomer **8a** can be eliminated as a possible structure. Two new signals, labeled as **11**, are observed in a 1:1 ratio. This is inconsistent with the formation of **8c** (mixed trimers).[28] On the basis of this data, we propose that the resting state of the catalyst is the dimer $[(pyr)Pd(OAc)_2]_2$ (**8b**).

Rate studies were next conducted to assess the order in each reaction component with $Pd(OAc)_2$/pyridine (1:1) as catalyst. Under these conditions, the reaction shows a half-order dependence on Pd (0.55 ± 0.02; Figure 15), a first-order dependence on benzene (0.94 ± 0.06; Figure 16), and a zero-order dependence on $PhI(OAc)_2$ (0.00 ± 0.06; Figure 17). In addition, a relatively large primary KIE (k_H/k_D = 3.9 ± 0.2) with C_6H_6/C_6D_6 is observed (Figure S28). These data are consistent with a mechanism in which a dimeric precatalyst (**8b**) enters the catalytic cycle by dissociation to a monomer (**5**) (Scheme 5). Rate-limiting C−H activation of benzene at **5** would then form the σ-aryl complex **6**, and fast oxidation and reductive elimination steps would release the product and regenerate the catalyst. The rate expression for the mechanism proposed in Scheme 5 can be derived as shown in eqs 10−13. It is in full accord with the experimental data.

DOI: 10.1021/jacs.5b00238
J. Am. Chem. Soc. 2015, 137, 3109−3118

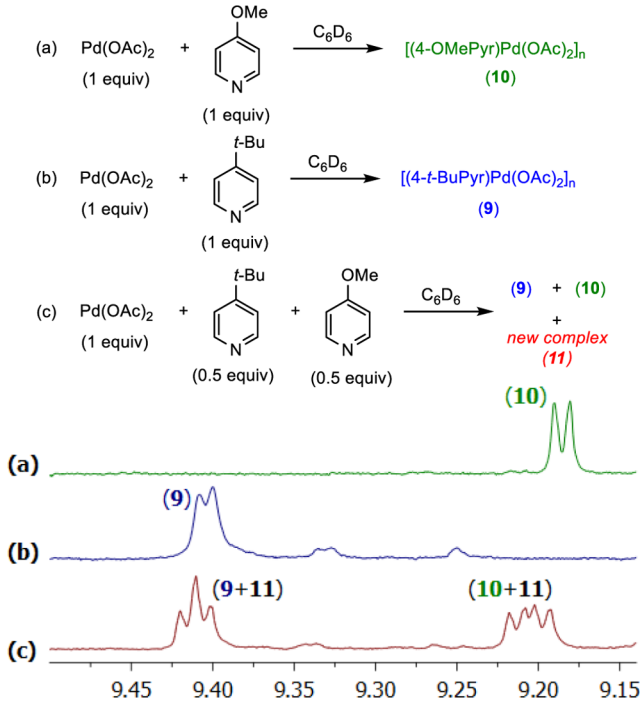

Figure 14. Mixed pyridines experiment. (a) Independently measured ^{1}H NMR spectrum when $Pd(OAc)_2$ and OMe-pyr (1:1) are mixed. (b) Independently measured ^{1}H NMR spectrum when $Pd(OAc)_2$ and *t*-Bu-pyr (1:1) are mixed. (c) ^{1}H NMR spectrum when $Pd(OAc)_2$, *t*-Bu-pyr, and OMe-pyr (1:0.5:0.5) are mixed. Two new peaks B and C are observed. (Spectra shown are the region corresponding to the signals of the 2-position of the monopyridine complexes. For full spectra, see Supporting Information, section 9).

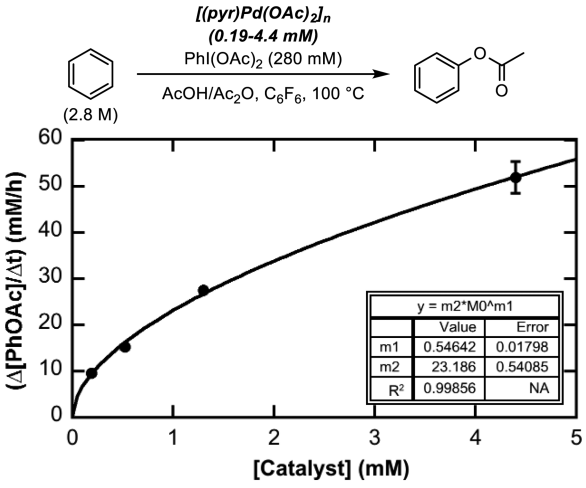

Figure 15. Plot of initial rate versus [Pd] with $Pd(OAc)_2$/pyr (1:1) as catalyst.

$$\text{rate} = \frac{\mathrm{d}(\text{PhOAc})}{\mathrm{d}t} = k_6[\text{benzene}][\mathbf{5}] \tag{10}$$

$$K_5 = \frac{[\mathbf{5}]}{[\mathbf{8b}]^{1/2}} \tag{11}$$

$$[\mathbf{5}] = K_5[\mathbf{8b}]^{1/2} \tag{12}$$

$$\text{rate} = k_6K_5[\text{benzene}][\mathbf{8b}]^{1/2} \tag{13}$$

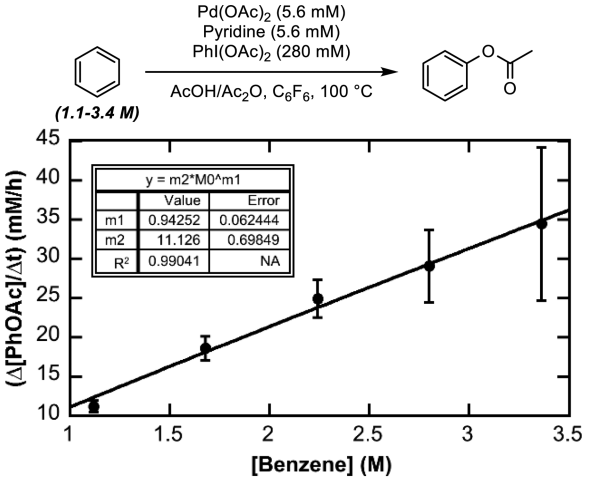

Figure 16. Plot of initial rate versus [benzene] with $Pd(OAc)_2$/pyr (1:1) as catalyst.

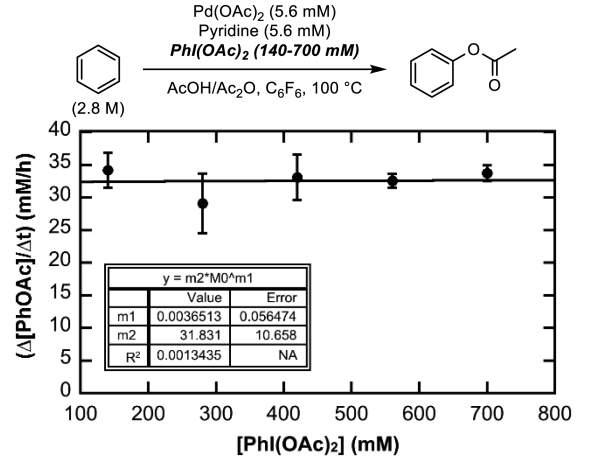

Figure 17. Plot of initial rate versus [$PhI(OAc)_2$] with $Pd(OAc)_2$/pyr (1:1) as catalyst.

Scheme 5. Proposed Mechanism with $Pd(OAc)_2$/pyr (1:1) as Catalyst

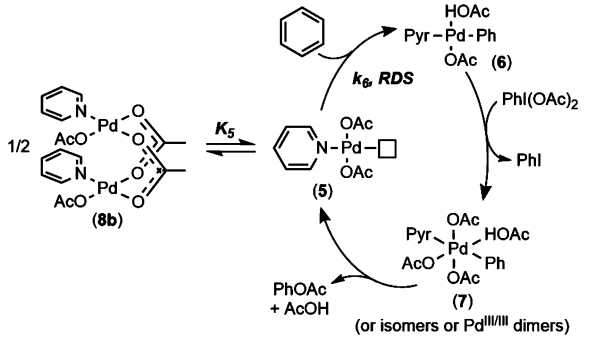

We next probed the impact of substituted pyridine ligands on the rate of the $Pd(OAc)_2$/pyridine (1:1) catalyzed C–H acetoxylation of benzene. As shown in the Hammett plot in Figure 18, substitution of the pyridine ligand had a negligible impact on the overall reaction rate ($\rho \sim 0$). This result can be rationalized based on counterbalancing electronic effects of pyridine substituents on the dissociation of dimer **8b-X** to monomer **5-X** (Scheme 6, step 1) and the coordination of benzene to form the η^2-benzene intermediate **12-X** (Scheme 6,

DOI: 10.1021/jacs.5b00238
J. Am. Chem. Soc. 2015, 137, 3109–3118

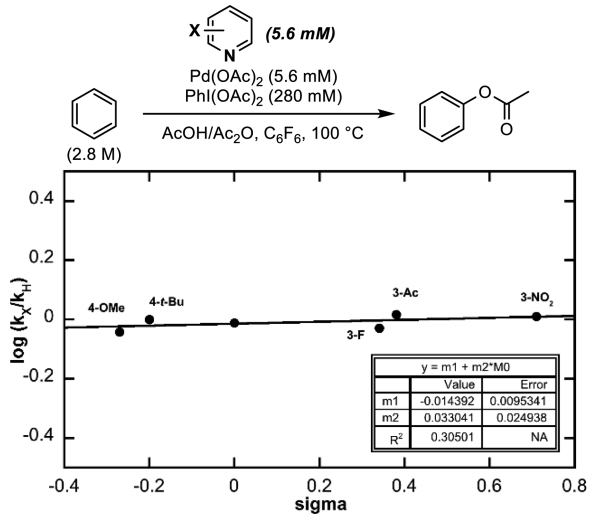

Figure 18. Hammett plot showing the effect of pyridine electronics with $Pd(OAc)_2$/pyr (1:1) as catalyst.

Scheme 6. Explanation for Lack of Pyridine Electronic Effect with Catalyst 8b

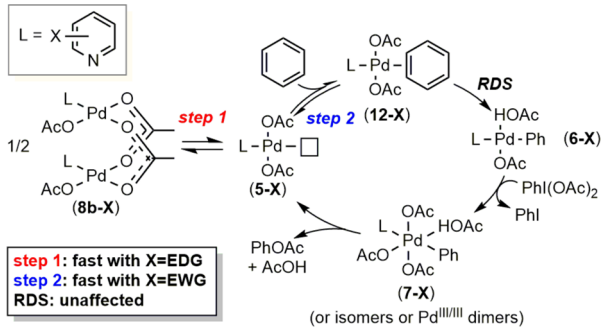

step 2). Step 1 is expected to be accelerated by electron-rich pyridine ligands[29] (e.g., 4-methoxypyridine), while step 2 is expected to be fastest with electron-deficient pyridines, such as 3-nitropyridine.[30] Rate-determining C−H activation would then occur at intermediate **12-X**. Literature precedent strongly suggests that this step proceeds via a concerted, acetate-assisted metalation-deprotonation transition state.[4] This transition state is cyclic, and minimal charge is accumulated. As such, we anticipate that substitution on the pyridine ligand would have minimal impact on the energy of this transition state. Overall, the observed Hammett ρ value of ∼0 is consistent with the electronic effects on steps 1 and 2 essentially canceling one another.

CONCLUSIONS

This article describes a detailed exploration of differences between three catalysts $Pd(OAc)_2$, $[(pyr)Pd(OAc)_2]_2$, and $(pyr)_2Pd(OAc)_2$ for the C−H acetoxylation of benzene. With all three catalyst systems, the reaction appears to involve rate-limiting C−H bond cleavage. NMR and kinetic studies suggest that the most active catalyst (**8**) rests as a dimer in solution. A comparison of the mechanisms with bis-pyridine complex **4** and monopyridine complex **8** implicates C−H activation occurring at the same intermediate **5**. The difference in reactivity between the bis- and monoligated catalysts, therefore, lies in how they enter into the catalytic cycle. Bis-pyridine complex **4** dissociates a pyridine ligand, while the dimeric monopyridine complex **8a** breaks up into a monomer. This study provides valuable insights into the chemistry of $Pd(OAc)_2$/pyr-based catalyst systems for C−H bond acetoxylation. Additionally, they have broader implications in catalysis, since Pd/pyr catalysts are employed for a variety of transformations including alcohol oxidation,[14a,d] alkene amination,[14b] indole arylation,[13c] and the Fujiwara−Moritani reaction.[13a,b]

ASSOCIATED CONTENT

Supporting Information

Experimental and spectral details for all new compounds as well as detailed experimental procedures and data for all kinetic and NMR experiments. This material is available free of charge via the Internet at http://pubs.acs.org.

AUTHOR INFORMATION

Corresponding Author

*mssanfor@umich.edu

Notes

The authors declare no competing financial interest.

ACKNOWLEDGMENTS

This work was supported by NSF under the CCI Center for Enabling New Technologies through Catalysis (CENTC) Phase II Renewal, CHE-1205189. A.K.C. thanks the Rackham Graduate School for a predoctoral fellowship. We thank Professors Tom Cundari, Karen Goldberg, Bill Jones, Elon Ison, and John Hartwig for valuable discussions. Dr. Marion H. Emmert is acknowledged for preliminary studies, particularly an initial DOSY experiment with $[(pyr)Pd(OAc)_2]_2$ as well as an initial investigation of pyridine electronic effects.

REFERENCES

(1) (a) Lyons, T. W.; Sanford, M. S. *Chem. Rev.* **2010**, *110*, 1147. (b) Muniz, K. *Angew. Chem., Int. Ed.* **2009**, *48*, 9412.

(2) (a) Noisier, A. F. M.; Brimble, M. A. *Chem. Rev.* **2014**, *114*, 8775. (b) Yamaguchi, J.; Yamaguchi, A. D.; Itami, K. *Angew. Chem., Int. Ed.* **2014**, *51*, 8960. (c) Wencel-Delord, J.; Glorius, F. *Nat. Chem.* **2013**, *5*, 369. (d) Chen, D. Y.-K.; Youn, S. W. *Chem. Eur, J.* **2012**, *18*, 9452. (e) Gutekunst, W. R.; Baran, P. S. *Chem. Soc. Rev.* **2011**, *40*, 1976. (f) McMurray, L.; O'Hara, F.; Gaunt, M. J. *Chem. Soc. Rev.* **2011**, *40*, 1885. (g) Godula, K.; Sames, D. *Science* **2006**, *312*, 67.

(3) For examples of mechanistic studies of ligand-directed Pd-catalyzed $C(sp^2)$−H functionalization, see: (a) Yang, Y.-F.; Cheng, G.-J.; Liu, P.; Leow, D.; Sun, T.-Y.; Chen, P.; Zhang, X.; Yu, J.-Q.; Wu, Y.-D.; Houk, K. N. *J. Am. Chem. Soc.* **2014**, *136*, 344. (b) Baxter, R. D.; Sale, D.; Engle, K. M.; Yu, J.-Q.; Blackmond, D. G. *J. Am. Chem. Soc.* **2012**, *134*, 4600. (c) Iglesias, Á.; Álvarez, R.; de Lera, Á. R.; Muñiz, K. *Angew. Chem., Int. Ed.* **2012**, *51*, 2225. (d) Powers, D. C.; Ritter, T. *Acc. Chem. Res.* **2012**, *45*, 840. (e) Ackermann, L. *Chem. Rev.* **2011**, *111*, 1315. (f) Lyons, T. W.; Hull, K. L.; Sanford, M. S. *J. Am. Chem. Soc.* **2011**, *133*, 4455. (g) Engle, K. M.; Wang, D.-H.; Yu, J. Q. *J. Am. Chem. Soc.* **2010**, *132*, 14137. (h) Powers, D. C.; Xiao, D. Y.; Geibel, M. A.; Ritter, T. *J. Am. Chem. Soc.* **2010**, *132*, 14530. (i) Deprez, N. R.; Sanford, M. S. *J. Am. Chem. Soc.* **2009**, *131*, 11234. (j) Powers, D. C.; Ritter, T. *Nat. Chem.* **2009**, *1*, 302. (k) Stowers, K. J.; Sanford, M. S. *Org. Lett.* **2009**, *11*, 4584. (l) Desai, L. V.; Stowers, K. J.; Sanford, M. S. *J. Am. Chem. Soc.* **2008**, *130*, 13285. (m) Li, J.-J.; Giri, R.; Yu, J.-Q. *Tetrahedron* **2008**, *64*, 6979. (n) Hull, K. L.; Lanni, E. L.; Sanford, M. S. *J. Am. Chem. Soc.* **2006**, *128*, 14047. (o) Yu, J.-Q.; Giri, R.; Chen, X. *Org. Biomol. Chem.* **2006**, *4*, 4041. (p) Kalyani, D.; Deprez, N. R.; Desai, L. V.; Sanford, M. S. *J. Am. Chem. Soc.* **2005**, *127*, 7330.

(4) For reviews of computational studies on the mechanism of CMD-type C−H activation, see: (a) Balcells, D.; Clot, E.; Eisenstein, O. *Chem. Rev.* **2010**, *110*, 749. (b) Lapointe, D.; Fagnou, K. *Chem. Lett.*

DOI: 10.1021/jacs.5b00238
J. Am. Chem. Soc. 2015, 137, 3109−3118

2010, *39*, 1118. (c) Boutadla, Y.; Davies, D. L.; Macgregor, S. A.; Poblador-Bahamonde, A. I. *Dalton Trans.* **2009**, 5820.

(5) For a review on methodological studies of C−H activation/functionalization with substrates that do not bear directing groups, see: (a) Kuhl, N.; Hopkinson, M. N.; Wencel-Delord, J.; Gloruis, F. *Angew. Chem., Int. Ed.* **2012**, *51*, 10236. For a subsequent report of C−H amination with substrates that do not bear directing groups, see: (b) Shrestha, R.; Mukherjee, P.; Tan, Y.; Litman, Z. C.; Hartwig, J. F. *J. Am. Chem. Soc.* **2013**, *135*, 8480. For subsequent reports on C−H arylation with substrates that do not bear directing groups, see: (c) Durak, L. J.; Lewis, J. C. *Organometallics* **2014**, *33*, 620. (d) Storr, T. E.; Namata, F.; Greaney, M. F. *Chem. Commun.* **2014**, *50*, 13275. (e) Wang, S.; Liu, W.; Cen, J.; Liao, J.; Huang, J.; Zhan, H. *Tetrahedron Lett.* **2014**, *55*, 1589. (f) Yan, T.; Zhao, L.; He, M.; Soulé, J.-F.; Bruneau, C.; Doucet, H. *Adv. Synth. Catal.* **2014**, *356*, 1586. (g) Zhao, L.; Yan, T.; Bruneau, C.; Doucet, H. *Catal. Sci. Technol.* **2014**, *4*, 352. (h) Cambeiro, X. C.; Boorman, T. C.; Lu, P.; Larrosa, I. *Angew. Chem., Int. Ed.* **2013**, *52*, 1781. (i) Wagner, A. M.; Sanford, M. S. *J. Am. Chem. Soc.* **2013**, *135*, 15110. (j) Ren, X.; Wen, P.; Shi, X.; Wang, Y.; Li, J.; Yang, S.; Yan, H.; Huang, G. *Org. Lett.* **2013**, *15*, 5194. (k) Storr, T. E.; Greaney, M. F. *Org. Lett.* **2013**, *15*, 1410. (l) Wencel-Delord, J.; Nimphius, C.; Wang, H.; Glorius, F. *Angew. Chem., Int. Ed.* **2012**, *51*, 13001. (m) Zhou, L.; Lu, W. *Organometallics* **2012**, *31*, 2124. For subsequent reports on C−H olefination with substrates that do not bear directing groups, see: (n) Gigant, N.; Bäckvall, J.-E. *Org. Lett.* **2014**, *16*, 4432. (o) Gigant, N.; Bäckvall, J.-E. *Org. Lett.* **2014**, *16*, 1664. (p) Jin, W.; Wong, W.-T.; Law, G.-L. *Chem. Catal. Chem.* **2014**, *6*, 1599. (q) Pham, M. V.; Cramer, N. *Angew. Chem., Int. Ed.* **2014**, *53*, 3484. (r) Vora, H. U.; Silvestri, A. P.; Engelin, C. J.; Yu, J.-Q. *Angew. Chem., Int. Ed.* **2014**, *53*, 2683. (s) Ying, C.-H.; Yan, S.-B.; Duan, W.-L. *Org. Lett.* **2014**, *16*, 500. (t) Zhou, L.; Lu, W. *Chem.—Eur. J.* **2014**, *20*, 634. (u) Min, M.; Choe, H.; Hong, S. *Asian J. Org. Chem.* **2012**, *1*, 47. (v) Wencel-Delord, J.; Nimphius, C.; Patureau, F. W.; Glorius, F. *Chem.—Asian J.* **2012**, *7*, 1208. For a subsequent report on C−H carboxylation with substrates that do not bear directing groups, see: (w) Suga, T.; Mizuno, H.; Takaya, J.; Iwasawa, N. *Chem. Commun.* **2014**, *50*, 14360.

(6) For mechanistic studies on C−H activation/functionalization with substrates that do not bear directing groups, see: (a) Cheng, C.; Hartwig, J. F. *J. Am. Chem. Soc.* **2014**, *136*, 12064. (b) Wang, D.; Izawa, Y.; Stahl, S. S. *J. Am. Chem. Soc.* **2014**, *136*, 9914. (c) Sanhueza, I. A.; Wagner, A. M.; Sanford, M. S.; Schoenebeck, F. *Chem. Sci.* **2013**, *4*, 2767. (d) Wagner, A. M.; Hickman, A. J.; Sanford, M. S. *J. Am. Chem. Soc.* **2013**, *135*, 15710. (e) Lyons, T. W.; Hull, K. L.; Sanford, M. S. *J. Am. Chem. Soc.* **2011**, *133*, 4455. (f) Tan, Y.; Hartwig, J. F. *J. Am. Chem. Soc.* **2011**, *133*, 3308. (g) Zhang, S.; Shi, L.; Ding, Y. *J. Am. Chem. Soc.* **2011**, *133*, 20218. (h) Hull, K. L.; Sanford, M. S. *J. Am. Chem. Soc.* **2009**, *131*, 9651. (i) Biswas, B.; Sugimoto, M.; Sakaki, S. *Organometallics* **2000**, *19*, 3895.

(7) For reviews summarizing various approaches to non-directed C−H functionalization, see: (a) ref 5a. (a) Neufeldt, S. R.; Sanford, M. S. *Acc. Chem. Res.* **2012**, *45*, 936. (b) Brückl, T.; Baxter, R. D.; Ishihara, Y.; Baran, P. S. *Acc. Chem. Res.* **2012**, *45*, 826. (b) Newhouse, T.; Baran, P. S. *Angew. Chem., Int. Ed.* **2011**, *50*, 3362. (c) Shul'pin, G. *Org. Biomol. Chem.* **2010**, *8*, 4217. (c) Ref 2g.. (d) Dick, A. R.; Sanford, M. S. *Tetrahedron* **2006**, *62*, 2439. For a perspective on the role of ligands in C−H activation, see: (e) Engle, K. M.; Yu, J.-Q. *J. Org. Chem.* **2013**, *78*, 8927.

(8) (a) Cook, A. K.; Emmert, M. H.; Sanford, M. S. *Org. Lett.* **2013**, *15*, 5428. (b) Gary, J. B.; Cook, A. K.; Sanford, M. S. *ACS Catal.* **2013**, *3*, 700. (c) Emmert, M. H.; Cook, A. K.; Xie, Y. J.; Sanford, M. S. *Angew. Chem., Int. Ed.* **2011**, *50*, 9409. (d) Emmert, M. H.; Gary, J. B.; Villalobos, J. M.; Sanford, M. S. *Angew. Chem., Int. Ed.* **2010**, *49*, 5884.

(9) For Pd-catalyzed C−H acetoxylation of arenes using $K_2S_2O_8$ as oxidant, see: (a) Eberson, L.; Jonsson, L. *Liebigs Ann. Chem.* **1977**, 233. (b) Eberson, L.; Jonsson, L. *Acta Chem. Scand. B* **1976**, *30*, 361. (c) Eberson, L.; Jonsson, L. *Acta Chem. Scand. B* **1974**, *28*, 771. (d) Eberson, L.; Jonsson, L. *J. Chem. Soc., Chem. Commun.* **1974**, 885.

(10) For Pd-catalyzed C−H acetoxylation of arenes using chromates, nitrogen oxides, and dioxygen as oxidants, see: ref 9a−c. (a) Eberson, L.; Gomez-Gonzales, L. *J. Chem. Soc. D* **1971**, 263. (b) Stock, L. M.; Tse, K.; Vorvick, L. J.; Walstrum, S. A. *J. Org. Chem.* **1981**, *46*, 1757. (c) Henry, P. M. *J. Org. Chem.* **1971**, *36*, 1886. (d) Tisue, T.; Downs, W. J. *J. Chem. Soc. D* **1969**, 410a. (e) Davidson, J. M.; Triggs, C. *J. Chem. Soc. A* **1968**, 1331.

(11) For related work on Pd-catalyzed C−H hydroxylation of arenes, see: (a) Guo, H.; Chen, Z.; Mei, F.; Zhu, D.; Xiong, H.; Yin, G. *Chem.—Asian J.* **2013**, *8*, 888. (b) Liang, P.; Xiong, H.; Guo, H.; Yin, G. *Catal. Commun.* **2010**, *11*, 560. (c) Lee, J. H.; Yoo, K. S.; Park, C. P.; Olsen, J. M.; Sakaguchi, S.; Prakash, G. K. S.; Mathew, T.; Jung, K. W. *Adv. Synth. Catal.* **2009**, *351*, 563. (d) Liu, Y.; Murata, K.; Inaba, M. *J. Mol. Catal. A* **2006**, *256*, 247. (e) Shibahara, F.; Kinoshita, S.; Nozaki, K. *Org. Lett.* **2004**, *6*, 2437. (f) Passoni, L. C.; Cruz, A. T.; Buffon, R.; Schuchardt, U. *J. Mol. Catal. A* **1997**, *120*, 117. (g) Jintoku, T.; Takaki, K.; Fujiwara, Y.; Fuchita, Y.; Hiraki, K. *Bull. Chem. Soc. Jpn.* **1990**, *63*, 438. (h) Jintoku, T.; Taniguchi, H.; Fujiwara, Y. *Chem. Lett.* **1987**, 1865.

(12) (a) Yoneyama, T.; Crabtree, R. H. *J. Mol. Catal. A* **1996**, *108*, 35. For subsequent work on Pd-catalyzed C−H acetoxylation using $PhI(OAc)_2$, see: (b) Tato, F.; García-Domínguez, A.; Cárdenas, D. J. *Organometallics* **2013**, *32*, 7487. (c) Wang, N.; McCormick, T. M.; Ko, S.-B.; Wang, S. *Eur. J. Inorg. Chem.* **2012**, 4463.

(13) (a) Kubota, A.; Emmert, M. H.; Sanford, M. S. *Org. Lett.* **2012**, *14*, 1760. (b) Zhang, Y.-H.; Shi, B.-F.; Yu, J.-Q. *J. Am. Chem. Soc.* **2009**, *131*, 5072. For an additional report in which a monopyridine/Pd complex is implied as an intermediate, see: (c) Stuart, D. R.; Fagnou, K. *Science* **2007**, *316*, 1172.

(14) (a) Steinhoff, B. A.; Stahl, S. S. *Org. Lett.* **2002**, *4*, 4179. For additional reports in which monopyridine/Pd complexes are implied as intermediates, see: (b) Ye, X.; Liu, G.; Popp, B. V.; Stahl, S. S. *J. Org. Chem.* **2011**, *76*, 1031. (c) Popp, B. V.; Stahl, S. S. *Chem.—Eur. J.* **2009**, *15*, 2915. (d) Schultz, M. J.; Adler, R. S.; Zierkiewicz, W.; Privalov, T.; Sigman, M. S. *J. Am. Chem. Soc.* **2005**, *127*, 8499.

(15) Stephenson, T. A.; Morehouse, S. M.; Powell, A. R.; Heffer, J. P.; Wilkinson, G. *J. Chem. Soc.* **1965**, 3632.

(16) Simmons, E. M.; Hartwig, J. F. *Angew. Chem., Int. Ed.* **2001**, *51*, 3066.

(17) Gary, J. B.; Sanford, M. S. *Organometallics* **2011**, *30*, 6143.

(18) Previous studies from our group suggested the possibility of interactions between the pyridine and hypervalent iodine oxidant [ref 3i]. To test this, varying mol fractions of 4-F-$PhI(OAc)_2$ and 3-fluoropyridine were combined in C_6D_6/CD_3CO_2D. However, ^1H and ^{19}F NMR spectroscopic analysis showed no changes in the chemical shifts of either species at room temperature or at 80 °C, indicating that there is no reaction between pyridine and the oxidant. See Supporting Information, section 7.

(19) Notably, complex **8** is not observed during catalysis when $Pd(OAc)_2$:Pyr (1:2) is used.

(20) Trend, R. M.; Ramtohul, Y. K.; Stoltz, B. M. *J. Am. Chem. Soc.* **2005**, *127*, 17778.

(21) Half order is observed when **4** is generated *in situ* (as in Figure 3) and when using the isolated complex **4** (see Supporting Information, section 6.5.4.).

(22) There is a possibility that **8** is the active catalyst under these conditions; however, because no signals corresponding to **8** are observed in the spectra of Figure 1a−c, this is an unlikely scenario. The possibility of **8** forming as an intermediate along the path from **4** to the RDS can not be not excluded.

(23) (a) Steinhoff, B. A.; Guzei, I. A.; Stahl, S. S. *J. Am. Chem. Soc.* **2004**, *126*, 11268. (b) King, A. E.; Ryland, B. L.; Brunold, T. C.; Stahl, S. S. *Organometallics* **2012**, *31*, 7948.

(24) Boller, T. M.; Murphy, J. M.; Hapke, M.; Ishiyama, T.; Miyaura, N.; Hartwig, J. F. *J. Am. Chem. Soc.* **2005**, *127*, 14263.

(25) By mass balance, $Pd(OAc)_2$ must also be formed under these conditions. However, this is likely also not the active catalyst because the rates of reactions with **8** are much higher than that with $Pd(OAc)_2$ alone.

DOI: 10.1021/jacs.5b00238
J. Am. Chem. Soc. 2015, 137, 3109−3118

(26) (a) Macchioni, A.; Ciancaleoni, G.; Zuccaccia, C.; Zuccaccia, D. *Supramolecular Chemistry: From Molecules to Nanomaterials*; Wiley: Hoboken, NJ, 2012; p 1. (b) Li, D.; Keresztes, I.; Hopson, R.; Willard, P. G. *Acc. Chem. Res.* **2009**, *42*, 270.
(27) For a review on the method of continuous variations, a related technique used to quantify aggregation, see: Renny, J. S.; Tomasevich, L. L.; Tallmadge, E. H.; Collum, D. B. *Angew. Chem., Int. Ed.* **2013**, *52*, 11998.
(28) The integral ratios also support formation of a dimer: two new signals labelled as **11** are observed in a 1:1 ratio; since the integral ratio of $[(4\text{-}t\text{-Bu-pyr})Pd(OAc)_2]_2$ and $[(4\text{-OMe-pyr})Pd(OAc)_2]_2$ is twice that of the mixed compound $(4\text{-}t\text{-Bu-pyr})(4\text{-OMe-pyr})Pd_2(OAc)_4$, the new complexes are formed in a 1:1:2 ratio (**9**:**10**:**11**), and this is consistent with the formation of **8b** (dimer).
(29) For a study on the trans influence as a function of pyridine substituents, see: Woods, C.; Daffron, C. *Inorg. Chim. Acta* **1985**, *101*, 13.
(30) Appleton, T. G.; Clark, H. C.; Manzer, L. E. *Coord. Chem. Rev.* **1973**, *10*, 335.

DOI: 10.1021/jacs.5b00238
J. Am. Chem. Soc. 2015, 137, 3109−3118